Influence of TiO$_2$ nano-particles on the transport properties of composite polymer electrolyte for lithium-ion batteries

C.W. Lin [a], C.L. Hung [b], M. Venkateswarlu [b], B.J. Hwang [b],*

[a] Department of Chemical Engineering, National Yunlin University of Science and Technology, Yunlin 640, Taiwan, ROC
[b] Department of Chemical Engineering, National Taiwan University of Science and Technology,
43 Keelung Road, Section 4, Taipei 106, Taiwan, ROC

Abstract

The influence of synthesized nano-sized TiO$_2$ particles on the ionic transport properties of PEO (polyethylene oxide)-based composite polymer electrolytes (CPEs) was investigated in this study. The nano-sized TiO$_2$ particles with pure anatase phase can be synthesized by a developed process. It was found that the ionic conductivity of the TiO$_2$ modified CPE increases with a decrease in the grain size of TiO$_2$. The conductivity ($\sigma = 1.40 \times 10^{-4}$ S cm^{-1}) for the PEO–10% LiClO$_4$–5% TiO$_2$ (3.7 nm) electrolyte is an order of magnitude higher than that the pure PEO–10% LiClO$_4$ ($\sigma = 1.03 \times 10^{-5}$ S cm^{-1}) at 30 °C. Meanwhile, the transference numbers of 0.51 and 0.21 were obtained for the TiO$_2$ modified CPE and pure PEO–LiClO$_4$, respectively. Both results imply that the nano-sized TiO$_2$ particles in the PEO–LiClO$_4$ matrix provide a new pathway for the transport of lithium ions.
© 2005 Elsevier B.V. All rights reserved.

Keywords: TiO$_2$; HMDS; IR; XRD; Conductivity; Transference number

1. Introduction

Studies on polymer electrolytes have been attracted great attention due to their potential applications for electric and load leveling vehicular applications [1,2]. PEO (polyethylene oxide)-based polymer electrolyte is of current interest for high energy density and high power lithium-ion batteries due to their easy formation of complex with lithium salts, high mobility of charge carriers, stable chemical properties, etc. [1]. The order of the conductivity of pure polyethylene oxide is around 10^{-7}–10^{-6} S cm^{-1} at room temperature [2–6] and the order of conductivity is not suitable for practical applications. The order of ionic conductivity of 10^{-6} to 10^{-4} S cm^{-1} was improved with the addition of various lithium salts (LiX; X = ClO$_4^-$, BF$_4^-$, PF$_6^-$, etc.) and liquid plasticizers like ethylene carbonate (EC) or propylene carbonate (PC) and low molecular weight polyethylene glycol (PEG) to the pure PEO polymer. However, the addition of liquid plasticizer

in the PEO–LiX polymer electrolyte can improve its ionic conductivity by an order of magnitude but their mechanical properties and potential stability of the films are not good for applications [7,8].

Recently, it has been reported that the addition of inorganic fillers like TiO$_2$, SiO$_2$ and Al$_2$O$_3$ nano-sized particles in the PEO–LiX polymer matrix improves its ionic conductivity and mechanical stability [2,3,5,6,9–11]. The TiO$_2$ with a particle size of 13 nm [2,10] and 21 nm [11–13] (from Degussa) is used to prepare the composite polymer electrolyte. Bloise et al. [14] have reported the effect of the TiO$_2$ particle size on the conductivity of the composite polymer electrolyte and the particle size of TiO$_2$ is larger than 19.7 nm in their study. Decreasing the particle size of inorganic TiO$_2$ fillers leads to enhance the interaction between the polymer matrix and inorganic fillers that might change the ionic conductivity of composite polymer electrolyte (CPE). To the best of our knowledge, no literature reports available on the influence of TiO$_2$ particle size in the range less than 10 nm on the transport properties of the composite polymer electrolyte. Therefore, it is of great interest to investigate

* Corresponding author. Tel.: +886 2 27376624; fax: +886 2 27376644.
E-mail address: bjh@ch.ntust.edu.tw (B.J. Hwang).

the influence of the nano-sized inorganic TiO_2 fillers with particle size less than 10 nm on the ionic conductivity of the CPE. To synthesize nano-sized TiO_2 particles, a process that the hydroxyl groups on the surface of TiO_2 precursor are eliminated by HMDS treatment is developed. The modified composite polymer electrolytes are obtained by adding the synthesized nano-sized TiO_2 particles into the PEO–$LiClO_4$ polymer matrix. The effect of grain/particle size of the synthesized TiO_2 on the ionic transport properties of PEO-based composite polymer electrolyte is investigated in this work.

2. Experimental

2.1. Preparation of TiO₂ powder

TiO_2 powders were prepared by a sol–gel process in which a proper amount of $TiCl_4$ (Acros) and ethanol (Acros) solvent were mixed and refluxed. The pH of solution mixture was adjusted to 7–8 by adding ammonia hydroxide. The solution become turbid and continued stirring till the formation of a high viscous gel. The gels were dried under vacuum at 70 °C for 24 h and the obtained flakes were pulverized to fine powder. The TiO_2 precursor obtained was treated with HMDS (Acros) vapors at 150 °C under nitrogen atmosphere [15] to eliminate its surface hydroxyl groups. The treated TiO_2 precursor was calcined at different temperatures to obtain nano-sized TiO_2 particles of various sizes.

2.2. Preparation of PEO-based polymer electrolyte

A stoichiometric amount of $LiClO_4$ (Acros) was dissolved in Tetrahydrofuron (THF) (Acros) solvent and stirred at room temperature. The TiO_2 nano-particles were dispersed in the solution mixture and the temperature of the dispersed mixture was raised to 70 °C. After 30 min of stirring, PEO (molecular weight: 600, 000) (Acros) was added to the solution and continued stirring for 24 h. The excess volatile organic solvent was evaporated upon continuous stirring and the solution become highly viscous and sticky in nature. An appropriate quantity of sticky solution was caste on the Teflon plate and vacuum dried at 60 °C for 24 h. The homogeneous and transparent polymer electrolyte film with an average thickness of 0.19 mm was obtained. The composite polymer electrolyte film was preserved in argon filled dry box (Mbraun, Unilab) in which the moisture and oxygen contents were maintained less than 1 ppm.

2.3. Characterization of TiO₂ powders by IR and XRD

The TiO_2 precursors were characterized by Infrared (IR) spectroscopy to confirm the elimination of hydroxyl groups on their surface. IR spectra were recorded using Bio-Rad (FTS-3500) spectrometer in the wavelength ranging from 2000 to 4000 cm^{-1}. The obtained TiO_2 powders were characterized by X-ray diffraction (Rigaku, Rotaflex X-ray

diffractometer) to evaluate the phase and grain size. The X-ray diffraction (XRD) pattern was recorded as intensity versus 2θ in the range of 20–60° at a scan rate of 5° min^{-1} using Cu Kα radiation. The grain size of TiO_2 was calculated using Scherrer's formula [16].

2.4. Ionic conductivity and Transference number measurements

Ionic conductivity of various PEO-based polymer electrolytes were measured using Solatron impedance analyzer (SI-1260) with electrochemical interface (SI-1286) at a wide frequency range (3 Hz–1.0 MHz) at different temperatures. In order to find the influence of particle size on the ionic conductivity, impedance measurements were performed on the CPE at different temperatures for various grain sizes of TiO_2 in the PEO–$LiClO_4$ polymer matrix. The ionic conductivity of various polymer electrolytes were determined using conductivity equation: $\sigma = t/(A \times R_b)$ S cm^{-1}; where σ is the conductivity, t is the thickness of the film, R_b and A are the resistance and cross-sectional area of the composite polymer electrolyte, respectively.

The transference number of lithium ions in the CPE was evaluated by applying dc potential across the symmetric cell of Li/PEO-based polymer electrolyte/Li and the initial and steady state current response of the cell was monitored for different time intervals. Ac impedance spectra were obtained before and after the polarization of the cell in order to estimate the impedance at the initial and steady state. Lithium transference number was determined using the modified formula [4,17]; $t^+ = I^s(\Delta V - I^0 R^0)/I^0(\Delta V - I^s R^s)$, where ΔV is the potential applied across the cell. I^0, I^s, R^0 and R^s are the initial and steady state interfacial currents and resistance, respectively.

3. Results and discussion

3.1. Synthesis and characterization of nano-sized TiO₂

The IR spectra of the HMDS treated and untreated TiO_2 precursors are presented in Fig. 1. The IR spectrum of HMDS untreated sample exhibited a broad band between the wave numbers of 2500 and 3400 cm^{-1} were assigned to the hydroxyl groups on the surface of the untreated TiO_2 precursor. This broad band was disappeared in the IR spectra of the HMDS treated TiO_2 precursor, implying that the developed process can successfully eliminate the hydroxyl groups on the surface of the TiO_2 precursor which may result in the grain growth of TiO_2 powders during sintering.

The untreated and treated TiO_2 powders were obtained from sintering the corresponding precursors. The XRD patterns of the untreated and treated TiO_2 powders at different sintering temperatures are presented in Fig. 2. The well-defined diffraction peaks are observed for the untreated TiO_2 powders calcined between 400 and 800 °C, implying
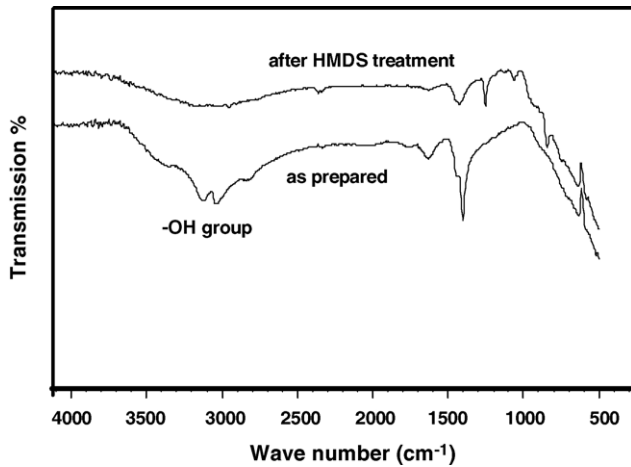
Fig. 1. IR spectra of TiO$_2$ powder as prepared and after HMDS treatment (a: anatase, r: rutile).

Fig. 3. The grain size of TiO$_2$ powders, as prepared and HMDS treated and sintered at various temperature.

the high degree of crystallinity of the untreated TiO$_2$ powders is obtained. The XRD pattern of TiO$_2$ powders as prepared and treated with HMDS are compared with JCPDS pattern of anatase and rutile phases of TiO$_2$ (Fig. 2). The XRD pattern indicates the existence of TiO$_2$ in anatase phase below 700 °C and the occurrence of phase transition from anatase to rutile phase at 700 °C and the coexistence of both anatse and rutile phase between 700 and 800 °C. The grain size of the untreated TiO$_2$ powder sintered at 700 °C for 1 h was found to be around 40 nm. The XRD patterns of the treated TiO$_2$ powders show larger peak width, implying that lower crystallinity and smaller grain size are obtained compared to the untreated TiO$_2$ powders. The grain size can be calculated from the Scherrer's formula for the HMDS treated and untreated TiO$_2$ powders and the variation of grain size with temperature are shown in Fig. 3. The average grain size of the treated TiO$_2$ powders increases insignificantly from 3.7 to 8.5 nm with

an increase in the sintering temperature from 400 to 800 °C. However, the grain size of the untreated TiO$_2$ powders is much larger and increases significantly (15.9–46.7 nm) as the sintering temperature increases from 500 to 800 °C. Meanwhile, only anatase phase was found even sintering at 800 °C. It suggests that the surface modification of TiO$_2$ is capable of impeding the phase transition from anatase to rutile (Fig. 2). The grain growth of the treated TiO$_2$ powders could be effectively inhibited with the HMDS treatment and also the aggregation of the treated TiO$_2$ powders could be avoided and result in better dispersion of the particles.

3.2. Transport properties of the PEO-based polymer electrolyte

In order to investigate the effect of particle size of TiO$_2$ on transport properties, the conductivity of the CPEs modified with various nano-sized particles of TiO$_2$ were obtained from the impedance measurements at 30 °C and at higher temperatures. It can be noticed that the ionic conductivity of the CPEs increases with a decrease in the grain size of TiO$_2$, implying their ionic conductivity can be improved by increasing the interfacial interaction between the TiO$_2$ and the PEO. The best conductivity of 1.40×10^{-4} S cm^{-1} was obtained at 30 °C for the PEO–10% LiClO$_4$–5% TiO$_2$ (3.7 nm). The Nyquist plots of the PEO–10% LiClO$_4$–5% TiO$_2$ for the smallest grain size (3.7 nm) of TiO$_2$ at various temperatures are shown in Fig. 4. The characteristics of the impedance spectra can be represented as an equivalent circuit in which an electrolyte resistance is in series with a parallel combination of an electrode resistance and a constant phase element as well as in series with a parallel combination of a Warburg resistance and a constant phase element [4]. The depressed semi-circle at high frequency and the slanted line at low frequency region in the impedance spectra represent the characteristics of the electrolyte resistance and Warburg resistance, respectively. The point of interception of a semi-circle on the real axis at
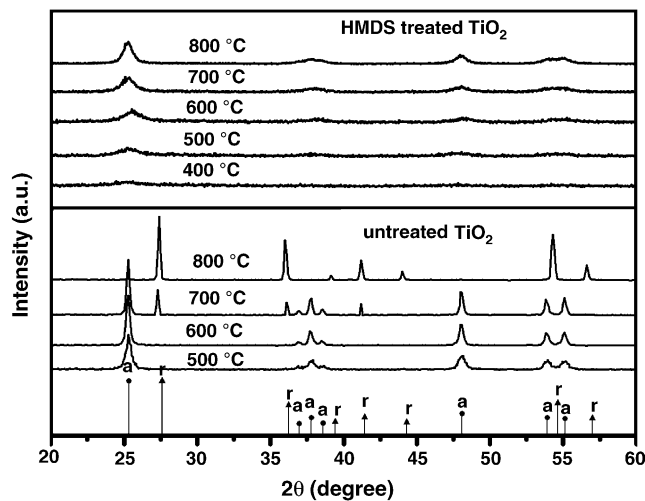

Fig. 2. XRD pattern of TiO$_2$, as prepared and HMDS treated at various sintering temperature and JCPDS pattern is also given for a comparison (a: anatase and r: rutile).
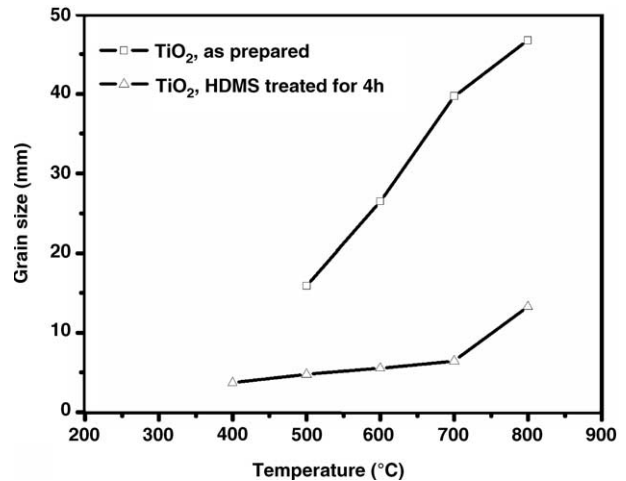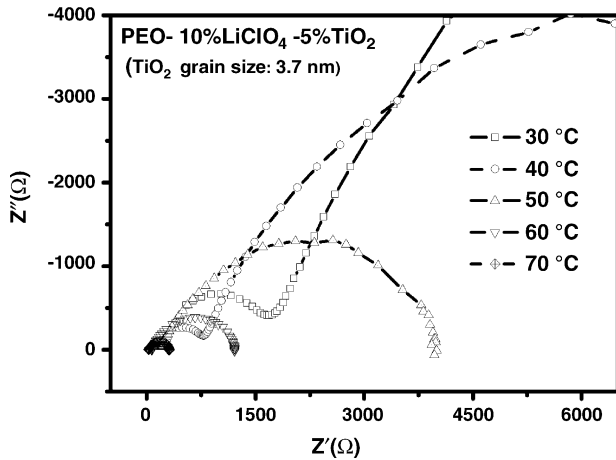
Fig. 4. The Nyquist plots of PEO–10% LiClO$_4$–5% TiO$_2$ at various temperatures.

Fig. 5. Temperature dependence conductivity plots of PEO–10% LiClO$_4$–Y% TiO$_2$ (Y = 0.0, 2, 5 and 8).

high frequency gives the electrolyte resistance of the CPE [4,5,18]. The conductivity data can be calculated from the measured electrolyte resistance from the impedance spectra and dimensions of the polymer electrolyte film (i.e., thickness and cross sectional area). The conductivity data for various PEO-based composite polymer electrolyte systems for different grain size of TiO$_2$ at 30 °C are presented in Table 1. From Table 1, it can be noticed that the ionic conductivity of the CPE is improved by addition of the TiO$_2$ particle size of 3.7 nm by an order and two orders of magnitude compared to that of the PEO–10% LiClO$_4$ ($\sigma = 1.03 \times 10^{-5}$ S cm^{-1}) and the pure PEO ($\sigma = 3.02 \times 10^{-6}$ S cm^{-1}) electrolytes, respectively. Meanwhile, the effect of TiO$_2$ particle size on the transport properties of the nano-composite polymer electrolyte is negligible if its size is larger than 22 nm (Table 1).

The temperature dependence of the ionic conductivity of the PEO-based composite polymer electrolytes was evaluated and the nature of plots are presented in Fig. 5. It can be noticed from Fig. 5 that the ionic conductivity for various nano-sized TiO$_2$ modified composite polymer electrolyte increases with an increase in TiO$_2$ content up to 5% and decreases for further increase of TiO$_2$ content. It may be due to the agglomeration of primary particles causing that the interaction between the nano-sized TiO$_2$ particles and PEO and also saturate the system [13] if the TiO$_2$ content is too high. It can be also seen from Fig. 5 that the ionic conductivity increases with increase of the temperature. The temperature dependence conductivity becomes insignificant at lower temperature range, implying
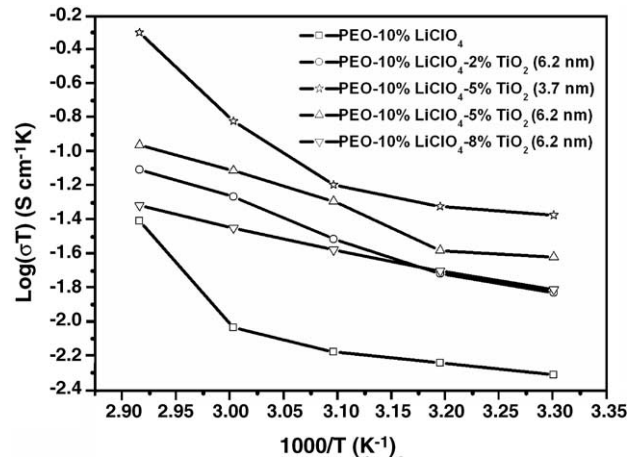
the contribution for ionic conduction from various pathways may change at different temperatures. From these observations, we can conclude that the improvement of ionic conductivity may result from the interaction between the nano-sized TiO$_2$ particles and PEO chains. Forsyth's group has found that the interactions of the Li$^+$–polymer and the polymer–TiO$_2$ but not the Li$^+$–TiO$_2$ in the composite polymer electrolyte [11,12]. However, we have observed the Li$^+$–TiO$_2$ environment in the polymer electrolyte modified with TiO$_2$ with smaller particles rather than larger particles. The variation of the contribution can be resolved by solid-state nuclear magnetic resonance (NMR) spectroscopy measurements will be presented in the forthcoming paper.

The variation of ionic conductivity of CPEs depends on the interaction between the cation with the nano-sized TiO$_2$ particles and oxygen in the PEO chain and also anions in the lithium salt. The interaction of TiO$_2$ nanoparticles with PEO segments and the ClO$_4^-$ anions induces structural modification of the polymer chain which provides favorable conduction path for faster migration of Li ion on the surface of the loaded TiO$_2$ nanoparticles [2,10]. Further, the interaction of nanoparticles with lithium salt and PEO chain renders the polymer in the amorphous phase even at moderate temperature. The restriction of crystallization and the increase of the amorphous phase could be considered as a possible reason for the higher mobility of charge carriers [5]. The interaction of TiO$_2$ nanoparticles with lithium salt and PEO chain promote a network with improved mechanical stability of the film [10]. The addition of the TiO$_2$ nanoparticles in

Table 1
Ionic conductivity (σ) and transference number (t^+) of PEO-based composite polymer electrolyte systems

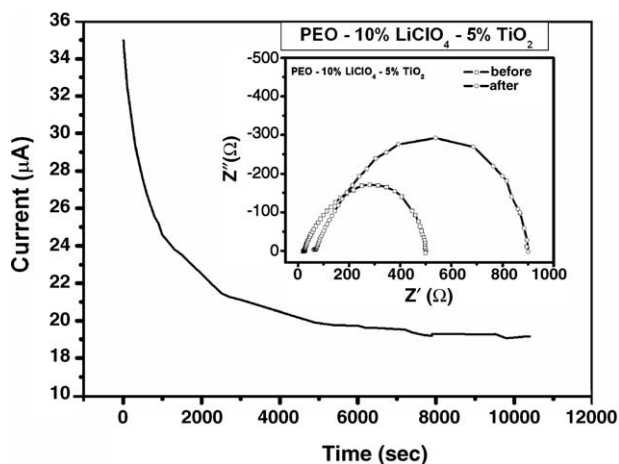| Electrolyte system	Conductivity (σ) (S cm^{-1}) at 30 °C	Transference number (t^+)
PEO (MW: 600000)	3.02×10^{-6}	–
PEO–10% LiClO$_4$	1.03×10^{-5}	0.21
PEO–10% LiClO$_4$–5% TiO$_2$(3.7 nm)	1.40×10^{-4}	0.51
PEO–10% LiClO$_4$–5% TiO$_2$(6.2 nm)	7.91×10^{-5}	–
PEO–10% LiClO$_4$–5% TiO$_2$ (22.0 nm)	1.40×10^{-5}	0.22

Fig. 6. dc polarization curve of the PEO–10% LiClO$_4$–5% TiO$_2$ (an inset figure shows the impedance spectra were obtained before and after the polarization of cell).

PEO–LiClO$_4$ could also prevent the re-crystallization in the PEO-based composite polymer electrolyte.

The current relaxation curve for the PEO–10% LiClO$_4$–5% TiO$_2$ composition is shown in Fig. 6 and the inset in Fig. 6 shows the impedance spectra were obtained before and after the polarization of the cell. The lithium transference number for the TiO$_2$ modified and un-modified polymer electrolytes was determined and data are given in Table 1. The transference numbers of 0.51 and 0.21, respectively, were obtained for the 5% of TiO$_2$ (3.7 nm) modified and un-modified polymer electrolytes. It suggests that the interaction of inorganic fillers and PEO chain with local relaxation and segmental motion, which promotes a favorable network for faster migration of the lithium ions. This in turn enhances the mobility of the lithium ions resulting in increase of lithium transference number and which is contributed for the improvement of ionic conductivity of the PEO-based composite polymer electrolyte.

4. Conclusion

A novel composite PEO-based polymer electrolyte was successfully obtained by the incorporation of the nano-sized TiO$_2$ particles synthesized by the developed process that can be eliminated the surface hydroxyl groups on the TiO$_2$ precursor. The grain growth of the TiO$_2$ can be inhibited through the HMDS treatment. The best ionic conductivity of 1.40×10^{-4} S cm^{-1} was obtained for the PEO–10%

LiClO$_4$–5% TiO$_2$ (3.7 nm) at 30 °C, which is an order of magnitude higher than that of the PEO–10% LiClO$_4$ electrolyte. The interaction between the loaded TiO$_2$ nanoparticles and PEO chain allow the structural modification which leads to faster migration of lithium ions in the CPEs. The enhancement of mobility of the lithium ions and flexible structure are responsible for the improvement of ionic conductivity of the CPE. The developed composite polymer electrolyte with high ionic conductivity and high lithium transference number can be used as a suitable membrane for solid state lithium-ion batteries.

Acknowledgements

References

[1] F.M. Gray, Solid Polymer Electrolytes: Fundamentals and Technological Applications, VCH, New York, 1991.
[2] F. Croce, G.B. Appetecchi, L. Persi, B. Scrosati, Nature 394 (1998) 456.
[3] B.K. Choi, Y.W. Kim, K.H. Shin, J. Power Sources 68 (1997) 357.
[4] K.M. Abraham, Z. Jiang, B. Corroll, Chem. Mater. 9 (1997) 1978.
[5] Y. Liu, J.Y. Lee, L. Hong, J. Appl. Poly. Sci. 89 (2003) 2815.
[6] W. Wieczorek, P. Lipka, G. Zukowska, H. Wycislik, J. Phys. Chem. B 102 (1998) 6968.
[7] Y.T. Kim, E.S. Smotkin, Solid State Ionics 149 (2002) 29.
[8] I. Nicotera, G.A. Panieri, M. Terenzi, A.V. Chadwick, M.I. Webster, Solid State Ionics 146 (2002) 143.
[9] C. Capiglia, P. Mustarelli, E. Quartarone, C. Tomasi, A. Magistris, Solid State Ionics 118 (1999) 73.
[10] F. Croce, R. Curini, A. Martinelli, L. Persi, F. Ronci, B. Scrosati, R. Caminiti, J. Phys. Chem. B 103 (1999) 10632.
[11] M. Forsyth, D.R. MacFarlane, A. Best, J. Adebahr, P. Jacobsson, A.J. Hill, Solid State Ionics 147 (2002) 203.
[12] A.S. Best, J. Adebahr, P. Jacobsson, D.R. MacFarlane, M. Forsyth, Macromolecules 34 (2001) 4549.
[13] N. Byrne, J. Efthimiadis, D.R. MacFarlane, M. Forsyth, J. Mater. Chem. 14 (2004) 127.
[14] A.C. Bloise, J.P. Donoso, C.J. Magon, A.V. Rosario, E.C. Pereira, Electrochim. Acta 48 (2003) 2239.
[15] N.L. Wu, S.Y. Wnag, I.A. Rusakova, Science 285 (1999) 1375.
[16] B.D. Cullity, S.R. Stock, Elements of X-Ray Diffraction, third ed., Prentice Hall, 2001, p. 170.
[17] J. Evans, C.A. Vincent, P.G. Bruce, Polymer 28 (1987) 2324.
[18] M. Watanabe, K. Sanui, N. Ogata, T. Kobayashi, Z. Ohtaki, J. Appl. Phys. 57 (1985) 123.